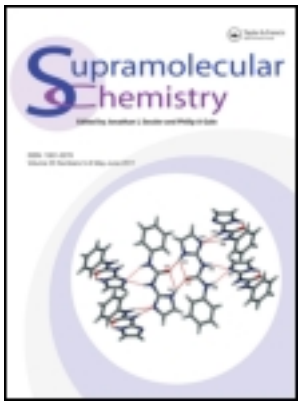

Supramolecular Chemistry
Publication details, including instructions for authors and subscription information:
http://www.tandfonline.com/loi/gsch20

Six new crystalline clathrates of cyclotricatechylene (CTC) including two donor-acceptor complexes

Jonathan J. Loughrey [a], Colin A. Kilner [a], Michaele J. Hardie [a] & Malcolm A. Halcrow [a]
[a] School of Chemistry, University of Leeds, Woodhouse Lane, Leeds, LS2 9JT, UK

Available online: 07 Oct 2011

To cite this article: Jonathan J. Loughrey, Colin A. Kilner, Michaele J. Hardie & Malcolm A. Halcrow (2012): Six new crystalline clathrates of cyclotricatechylene (CTC) including two donor-acceptor complexes, Supramolecular Chemistry, 24:1, 2-13

To link to this article: http://dx.doi.org/10.1080/10610278.2011.611246

Supramolecular Chemistry
Vol. 24, No. 1, January 2012, 2–13

Taylor & Francis
Taylor & Francis Group

Six new crystalline clathrates of cyclotricatechylene (CTC) including two donor–acceptor complexes

Jonathan J. Loughrey, Colin A. Kilner, Michaele J. Hardie* and Malcolm A. Halcrow*

School of Chemistry, University of Leeds, Woodhouse Lane, Leeds LS2 9JT, UK

(*Received 27 June 2011; final version received 23 July 2011*)

Dark blue $[CTC]_2$·(TCNE)·6THF and dark green $[CTC]_2$·(TCNQ)·4THF are both exclusion complexes, with the cyanoalkene acceptor being sandwiched between the catechol rings of two cyclotricatechylene (CTC) host molecules. There is also extensive hydrogen bonding between the CTC and tetracyanoethene (TCNE) or tetracyanoquinodimethane (TCNQ) molecules, which is unusual for crystals containing these cyanoalkenes. Crystallographic, IR and UV–vis data show that these are typical donor–acceptor complexes, with strong charge–transfer interactions between the CTC and cyanoalkene acceptors. These are the first donor–acceptor complexes of a cyclotriveratrylene (CTV)-derived host, and the first crystallographically characterised adducts between TCNE or TCNQ and an organic cavitand. The solvate CTC·3.5THF·0.5H_2O adopts a novel nanoporous crystal lattice, composed of undulating hydrogen-bonded sheets of CTC molecules. In contrast, the clathrates CTC·2EtOH, CTC·3DMA and CTC·5DMSO all adopt structures that are related to previously reported clathrates of CTC, containing hydrogen-bonded bilayers or *bis*-monolayers of CTC molecules. The CTC molecules in all six structures contain included guest solvent. This contrasts with CTV clathrate crystals, which rarely contain included solvent.

Keywords: cyclotricatechylene; cavitand; donor–acceptor complex; crystal engineering

Introduction

Cyclotriveratrylene (CTV) is one of the most important cavitand hosts in supramolecular chemistry, both in its own right (*1*, *2*) and as a scaffold for the construction of derivatives with extended cavities, organic capsules (cryptophanes) (*3*) and metal-organic capsules and other architectures (*2*). In the crystalline state, CTV forms in-cavity complexes with fullerenes and some other globular molecules, but usually forms exclusion clathrates with solvents or other small molecules (*1*, *2*). However, extended cavitands and capsules containing the CTV core have a much more varied inclusion chemistry, complexing a range of small organic molecules and even gases (*2*, *3*).

The *tris*-catechol analogue cyclotricatechylene (CTC) is obtained in one step by demethylation of CTV (*4*), but has been little studied by comparison (Scheme 1). There are four previously published clathrate materials of CTC with organic solvents, which have varying stoichiometries (*4–6*). Three of these adopt a similar crystal packing motif in which the CTC molecules and solvent associate with hydrogen-bonded bilayers, with alternating 'up' and 'down' CTC cavities. The connectivity of the CTC nodes in the hydrogen bonding topology of the bilayers varies between the structures, however, depending on the number of solvent molecules present and their hydrogen bonding character. The exception to this generalisation is CTC·2DMF·2H_2O, which forms an alternative lattice type containing sheets of DMF solvent encapsulated by an 'up' and a 'down' monolayer of hydrogen-bonded CTC molecules (*7*). In addition to taking part in the hydrogen bond network, one equivalent of solvent is always included in the CTC host cavity in these structures. This implies that CTC may be a stronger host for small molecules in the solid state than CTV, whose clathrate crystals rarely contain in-cavity solvent. A small number of metal complexes of CTC have also been reported, some of which also contain included solvent (*8*, *9*).

Given the continued interest by some of us in the supramolecular chemistry of CTV derivatives (*2*, *10*, *11*), we have examined the host–guest chemistry of CTC in more detail. Although the electrochemistry of CTC itself has not been described, in complexed form its catechylene groups are redox active (*8*) as expected for a catecholate derivative (*12*). Hence electron-acceptor guests were of particular interest, since these have potential to form donor–acceptor or charge-transfer complexes with CTC (*13–15*). With that in mind, we report here the crystalline adducts of CTC with tetracyanoethene (TCNE) and tetracyanoquinodimethane (TCNQ), together with four

*Corresponding authors. Email: m.j.hardie@leeds.ac.uk; m.a.halcrow@leeds.ac.uk

ISSN 1061-0278 print/ISSN 1029-0478 online

http://dx.doi.org/10.1080/10610278.2011.611246
http://www.tandfonline.com

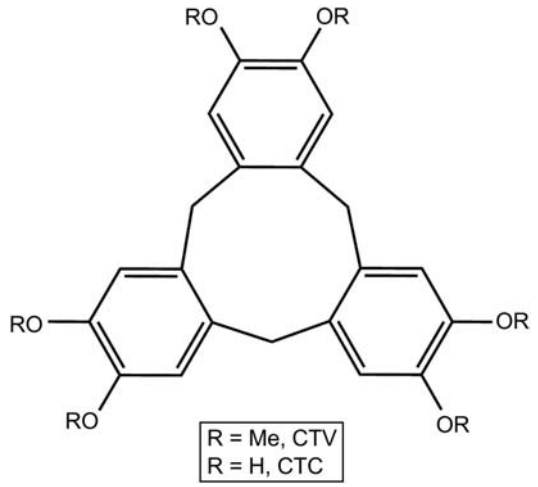

Scheme 1. Structures of cyclotriveratrylene (CTV) and cyclotricatechylene (CTC).

other CTC clathrate structures that we also obtained during this work. Some TCNE and TCNQ complexes of calixarene (*16*) and resorcinarene (*17–19*) derivatives have been determined spectroscopically in solution, but this report contains the first crystal structure determinations of TCNE or TCNQ complexes with any of the important classes of organic cavitand.

Experimental

CTC was prepared by the literature method (*4*), and all reactions and crystallisations were performed using as-supplied AR-grade solvents. Elemental microanalyses were performed by the University of Leeds School of Chemistry microanalytical service. Infrared spectra were obtained as KBr discs between 400–4000 cm^{-1}, using a Nicolet Avatar 360 spectrophotometer. Electrospray mass spectra (ES-MS) were obtained on a Waters ZQ4000 spectrometer from THF feed solutions. UV–vis spectra were run on a PerkinElmer Lambda900 spectrophotometer using 1 cm quartz cells.

Syntheses

Slow diffusion of pentane vapour into THF solutions of CTC and TCNE or TCNQ yielded large dark blue blocks of $[CTC]_2$·TCNE·6THF (**1**) or dark green needles of $[CTC]_2$·TCNQ·4THF (**2**). The latter material was always contaminated by colourless crystals of CTC·3.5THF·0.5H_2O (**3**), which were separated manually for analysis. The other clathrates CTC·2EtOH (**4**), CTC·3DMA (**5**) and CTC·5DMSO (**6**) were grown by slow diffusion of diethyl ether vapour into solutions of CTC in the relevant solvent.

Characterisation data for **1**. Found C, 65.5; H, 5.50; N, 5.1%. Calcd for $C_{48}H_{36}N_4O_{12}$·3$[C_4H_8O]_3$·H_2O C 65.8; H 5.71; N 5.1%. ES-MS *m/z* 175.1 (11%, $[Na_3(CTC)(H_2O)_5]^{3+}$), 215.1 (100%, $[Na_2(CTC)(H_2O)]^{2+}$), 230.8 (16%, $[Na_2(CTC)(THF)]^{2+}$), 285.1 (34%, $[Na(CTC)(THF)_2(H_2O)_2 + H]^{2+}$), 317.1 (69%, $[Na_3(CTC)(THF)_2(H_2O)_3 + H]^{2+}$), 407.2 (19%, $[Na(CTC)(H_2O)]^{+}$), 611.3 (13%, $[Na(CTC)(THF)_2(H_2O)_2(MeCN)]^{+}$). Negative ion ES-MS *m/z* 249.0 (39%, $[Na(CTC)(O_2CH)_2(H_2O)]^{2-}$), 311.1 (18%, $[Na_2(CTC)(TCNE)(OH_2)_2 + H]^{-}$), 365.1 (13%, $[CTC—H]^{-}$), 411.1 (51%, $[(CTC)(O_2CH)]^{-}$), 469.2 (100%, $[Na(CTC)(O_2CH)(OH_2)(OH)]^{-}$), 495.1 (24% $[(CTC)(TCNE) + H]^{-}$), 731.2 (12%, $[(CTC)_2—H]^{-}$). IR (KBr disc) 3338br s, 3055w, 2989w, 2924w, 2878w, 2249w, 2238w, 2220w, 1613s, 1515s, 1479m, 1446s, 1362s, 1282m, 1236s, 1186m, 1171m, 1133s, 1071m, 1024m, 940m, 931m, 889m, 856s, 821w, 787w, 748m, 706w, 666w, 641w, 618m, 568m, 524w cm^{-1}. UV–vis (THF) λ_{max}, nm (ε_{max}, 10^3 dm^3 mol^{-1} cm) 261 (41.1), 290 (12.5), 330 (sh), 655 (0.2).

Characterisation data for **2**. Found C, 67.6; H, 5.85; N, 4.3%. Calcd for $C_{54}H_{40}N_4O_{12}$·3$[C_4H_8O]_3$·H_2O C, 67.7; H, 5.68; N, 4.8%. Positive ion ES-MS *m/z* 175.1 (6%, $[Na_3(CTC)(H_2O)_5]^{3+}$), 215.1 (100%, $[Na_2(CTC)(H_2O)]^{2+}$), 230.8 (14%, $[Na_2(CTC)(THF)]^{2+}$), 285.2 (10%, $[Na(CTC)(THF)_2(H_2O)_2 + H]^{2+}$), 317.2 (69%, $[Na_3(CTC)(THF)_2(H_2O)_3 + H]^{2+}$), 407.2 (19%, $[Na(CTC)(H_2O)]^{+}$), 611.3 (13%, $[Na(CTC)(THF)_2(H_2O)_2(MeCN)]^{+}$). Negative ion ES-MS *m/z* 195.0 (96%, $[(NC)_2C{=}C_6H_4{=}C(CN)(OH)]^{-}$), 204.0 (100%, $[TCNQ]^{-}$). IR (KBr disc) 3412br m, 3047w, 2979w, 2694w, 2344br w, 2219m, 2186w, 1604m, 1543m, 1518s, 1477m, 1444s, 1356m, 1282s, 1196w, 1173m, 1131m, 1070m, 1044m, 938wm, 930w, 884m, 858m, 844w, 788w, 745m, 705w, 668w, 616m, 566w, 523w cm^{-1}. UV–vis (THF) λ_{max}, nm (ε_{max}, 10^3 dm^3 mol^{-1} cm) 290 (26.8), 380 (sh), 405 (31.4), 490 (5.2), 725 (0.08).

Crystal structure determinations

Experimental details of the structure determinations are given in Table 1. All diffraction data were measured using a Bruker X8 Apex diffractometer, with graphite-monochromated Mo-K_α radiation ($\lambda = 0.71073$ Å) generated by a rotating anode. The diffractometer was fitted with an Oxford Cryostream nitrogen low temperature device. The structures were solved by direct methods using *SHELXS97* (*19*), and developed by full least-squares refinement on F^2 (*SHELXL97*) (*20*). Crystallographic figures were prepared using *X-SEED* (*21*). The definitions of the symmetry codes in the crystallographic figures and table are collected in Table 2.

The asymmetric unit of **1** contains two CTC molecules; two half-molecules of TCNE spanning the crystallographic inversion centres 0,1/2,0 and 1,0,1/2 and six molecules of THF. No disorder was detected during the refinement. All non-H atoms were refined anisotropically,

Table 1. Experimental details for the crystal structures in this work.

	[CTC]$_2$·TCNE·6THF (**1**)	[CTC]$_2$·TCNQ·4THF (**2**)	CTC·3.5THF·0.5H$_2$O (**3**)	CTC·2EtOH (**4**)	CTC·3DMA (**5**)	CTC·5DMSO (**6**)
Formula	$C_{72}H_{84}N_4O_{18}$	$C_{70}H_{72}N_4O_{16}$	$C_{35}H_{47}O_{10}$	$C_{25}H_{30}O_8$	$C_{33}H_{45}N_3O_9$	$C_{31}H_{48}O_{11}S_5$
fw	1293.43	1225.32	627.73	458.49	627.72	756.99
Crystal system	Triclinic	Monoclinic	Monoclinic	Triclinic	Monoclinic	Triclinic
Space group	$P\bar{1}$	$C2/c$	$P2_1/c$	$P\bar{1}$	$P2_1/n$	$P\bar{1}$
a (Å)	8.4993(8)	36.991(4)	17.0327(18)	9.7892(13)	10.6929(11)	10.7307(15)
b (Å)	19.5382(18)	8.4427(7)	17.7830(19)	9.8054(12)	29.946(3)	13.8053(19)
c (Å)	20.2820(19)	21.661(3)	11.0070(10)	13.4571(17)	10.8181(11)	13.9949(18)
α (°)	90.463(4)	–	–	95.622(6)	–	73.045(6)
β (°)	92.464(5)	118.233(7)	91.371(4)	93.690(7)	103.744(4)	75.117(6)
γ (°)	95.706(4)	–	–	106.325(7)	–	81.243(6)
V (Å^3)	3348.0(5)	5960.0(12)	3333.0(6)	1227.9(3)	3364.9(6)	1909.9(4)
ρ_{calc} (g cm^{-3})	1.283	1.366	1.251	1.240	1.239	1.316
Z	2	4	4	2	4	2
T (K)	150(2)	150(2)	150(2)	150(2)	150(2)	150(2)
μ Mo-K_α (mm^{-1})	0.092	0.097	0.091	0.092	0.090	0.356
No. of reflections	105133	89496	37625	44830	45901	80977
Unique reflections	17469	8914	8021	7225	8582	11108
R_{int}	0.069	0.067	0.066	0.073	0.141	0.056
Parameters/restraints	884/12	452/28	444/50	333/8	440/6	463/6
R_1 ($I > 2\sigma$ (I))	0.073	0.067	0.081	0.047	0.060	0.051
wR_2 (all data)	0.207	0.188	0.270	0.134	0.183	0.138
GOF	1.052	1.050	1.025	1.061	1.041	1.036
Largest Fourier peak/hole (e Å^{-3})	1.18/−0.72	1.16/−0.55	0.73/−0.33	0.32/−0.37	0.40/−0.38	2.56/−0.87

Table 2. Definitions of the symmetry codes in the discussions of the crystal structures in this work.

(i)	$2-x, -y, 1-z$	(ix)	$1/2-x, 7/2-y, 1-z$
(ii)	$-x, 1-y, -z$	(x)	$1/2-x, -1/2+y, 1/2-z$
(iii)	$-x, 1-y, 1-z$	(xi)	$x, 2-y, 1/2+z$
(iv)	$-2+x, 1+y, z$	(xii)	$-x, y, 1/2-z$
(v)	$-2-x, 2-y, -z$	(xiii)	$1/2-x, 1/2+y, 1/2-z$
(vi)	$2+x, -1+y, z$	(xiv)	$x, 3-y, 1/2+z$
(vii)	$1+x, y, z$	(xv)	$x, 1+y, z$
(viii)	$1-x, -y, 1-z$	(xvi)	$1/2-x, 5/2-y, 1-z$

and C-bound H atoms were placed in calculated positions and refined using a riding model. The hydroxyl H atoms were located in the Fourier map and refined with a common U_{iso} thermal parameter of 0.062(3), subject to the fixed restraint O—H = 0.90(2) Å. The maximum residual Fourier peak of $+1.2\,e$ Å^{-3} is 1.1 Å from the solvent C atom C(77), and may indicate a minor degree of disorder in that residue. This was not modelled, however.

The structure of **2** was solved in the space group $P\bar{1}$, then transformed up to $C2/c$ using the *ADSYMM* routine in *PLATON* (*22*). The asymmetric unit contains one CTC molecule; one half-molecule of TCNQ spanning the crystallographic inversion centre 1/4, 7/4, 1/2; and two molecules of THF, one of which was disordered. The disordered molecule was modelled over two sites with refined occupancies of 0.59:0.41, and the refined restraints C—O = C—C = 1.44(2) and 1,3-C···O = 1,3-C···C = 2.35(2) Å. All non-H atoms except the minor solvent disorder site were refined anisotropically, and C-bound H atoms were placed in calculated positions and refined using a riding model. The hydroxyl H atoms were located in the Fourier map and refined subject to the fixed restraint O—H = 0.90(2) Å, with a thermal parameter of $1.2\times$ U_{eq} for the corresponding O atom. For O(7), O(8), O(16) and O(25), two different hydroxyl H atom sites were identified in the Fourier map, consistent with the consequences of a hydrogen bond involving O(16) that is disordered about a crystallographic C_2 axis. These were included in the model, with arbitrary half-occupancies for each partial H atom. Steric considerations imply that there should also be a second partial site for H(26), but this was not located in the Fourier map. The maximum residual Fourier peak of $+1.2\,e$ Å^{-3} lies within the disordered solvent area.

The asymmetric unit of **3** contains one CTC molecule; two ordered and wholly occupied THF molecules; one disordered region of solvent that was modelled as three equally occupied THF molecules; and, another disordered

region spanning the inversion centre at 0, 1/2, 0 that was refined as two 1/4-occupied THF sites and a half molecule of water. Presumably one side of the inversion centre is occupied by disordered THF and the other side by water, with a random distribution of the two through the crystal. The half-water molecule O(43) is within hydrogen bonding distance of the CTC molecule, which lends some support to that interpretation. The triply disordered THF molecule C(38)—C(42) was modelled as three equally occupied C_5 rings. This region of the Fourier map occupies channels running parallel to the unit cell *c*-axis and is poorly defined, so it was not possible to distinguish the C and O atoms in these partial THF sites. The other, doubly disordered half-THF molecule O(44)—C(48) was better resolved, and was refined with distinct C and O atoms. The refined restraints C-C = C-O = 1.45(2) and 1,3-C···C = 1,3-C···O = 2.37(2) Å were applied to these disordered residues. All wholly occupied non-H atoms were refined anisotropically. H atoms were placed in calculated positions and refined using a riding model, except for the triply disordered THF and partial water sites. Their H atoms were not included in the final model, but were included in the density and *F*(000) calculations.

The asymmetric units of all the other CTC clathrate crystals contain one formula unit, with minor solvent disorder. One of the two ethanol methyl groups in **4** is disordered over two sites with refined occupancy 0.60:0.40. In **5**, disorder was seen in the carbonyl C and N atoms of one of the three DMA solvent molecules. These two atoms were modelled over two orientations without restraints, and with refined occupancies of 0.78:0.22. Finally, one of the five unique DMSO sites in **6** was found to be disordered, over two sites with a refined occupancy ratio of 0.68:0.32. These partial DMSO molecules were modelled without restraints, using a common wholly occupied O atom. All non-H atoms were refined anisotropically in these structures, except for the minor solvent disorder sites in **5** and **6**, and C-bound H atoms were placed in calculated positions and refined using a riding model. The hydroxyl H atoms in all the structures were located in the Fourier map and refined with a common U_{iso} thermal parameter, subject to the fixed restraint O—H = 0.90(2) Å. The highest residual Fourier peak of $+2.6\,e$ Å^{-3} in **6** lies within the disordered DMSO molecule, and probably indicates a third, minor disorder site for this residue. There are no noteworthy residual Fourier peaks or troughs in **4** and **5**.

Results and discussion

Addition of the cyanoalkenes TCNE, TCNQ, 2,3-dichloro-4,5-dicyanobenzoquinone or *N*,*N*′-dicyano-2,5-dimethylbenzoquinonediimine to CTC in organic solvents yields intense blue, green or orange solutions that indicate the formation of donor–acceptor complexes. These coloured solutions often bleach over a period of 1 or 2 days, making

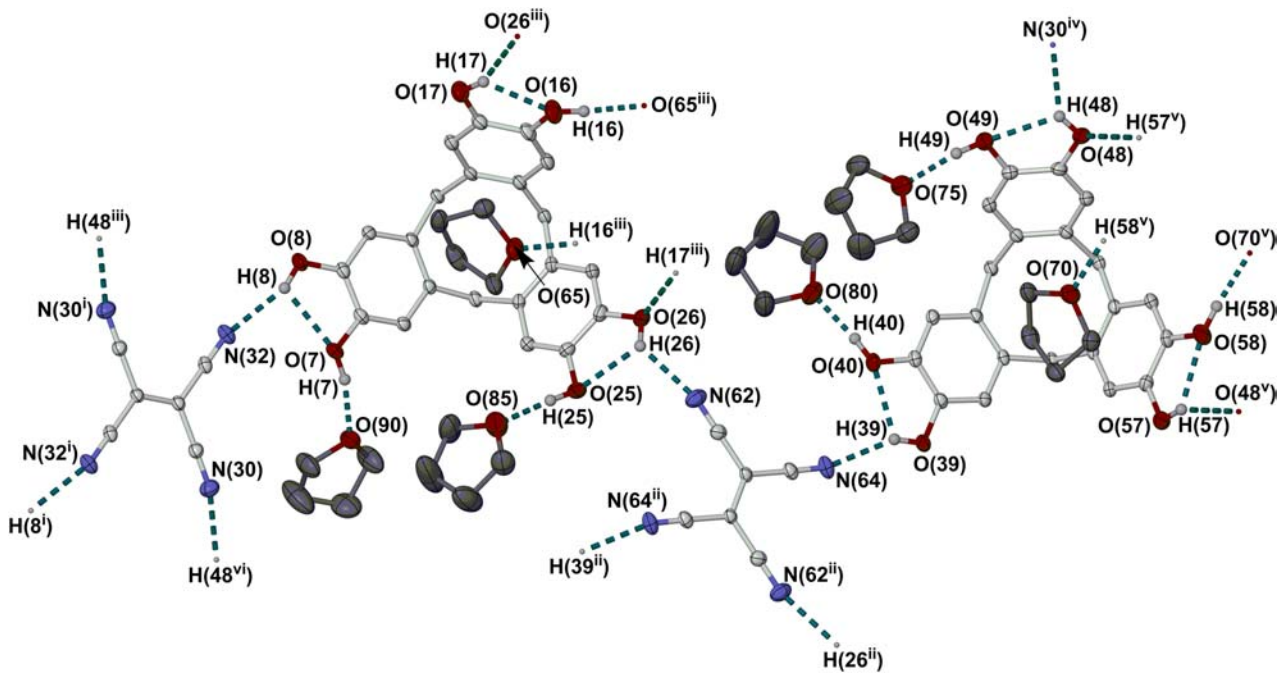

Figure 1. View of the asymmetric unit of **1**, showing the hydrogen bonding interactions in the crystal. For clarity, the C-bound H atoms have been omitted, and only the atoms involved in hydrogen bonding have been labelled. Displacement ellipsoids are at the 50% probability level. See Table 2 for the definitions of the symmetry codes. The same atom numbering scheme for the CTC molecule on the left is also used in the other clathrate structures.

them difficult to crystallise. This probably reflects hydrolysis of the cyanoalkene reagents in the undried solvents used (*13*, *18*, *23*), since unchanged CTC was crystallised from several of the bleached solutions (see below). The complexes appeared to be the most stable in THF, out of the solvents we examined, and slow diffusion of pentane vapour into those TCNE- or TCNQ-containing solutions reproducibly yielded large dark blue blocks of formula $(CTC)_2$·TCNE·6THF (**1**) or dark green needles of $(CTC)_2$·TCNQ·4THF (**2**). Samples of **2** are always contaminated by colourless crystals, from which it must be separated manually for analysis. This impurity was identified as the THF solvate CTC·3.5THF·0.5H_2O (**3**), which is described below. Compound **3** can also be obtained in pure form by crystallising CTC from THF/Et_2O in the absence of TCNQ.

The asymmetric unit of **1** contains two molecules of CTC and two half-molecules of TCNE spanning crystallographic inversion centres (Figure 1). Each molecule of CTC donates hydrogen bonds to two different TCNE molecules and one other molecule of CTC, and to three THF solvent molecules. These hydrogen bonding interactions associate with the CTC and TCNE molecules into a puckered 2D sheet running parallel to the crystallographic

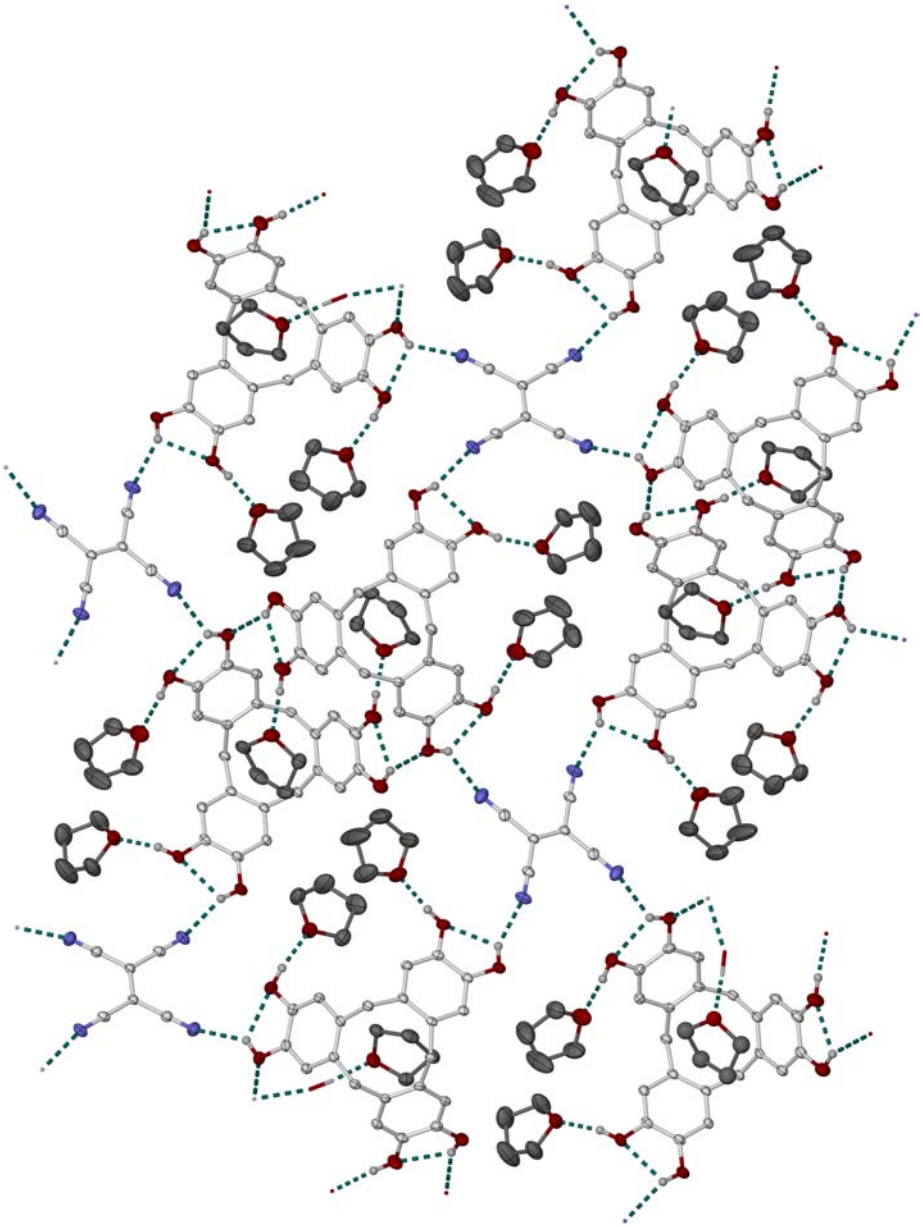

Figure 2. View of the puckered 2D network formed by the hydrogen bonds in **1**. The view is perpendicular to the (120) crystal plane. Displacement ellipsoids are at the 50% probability level, and all C-bound H atoms have been omitted for clarity.

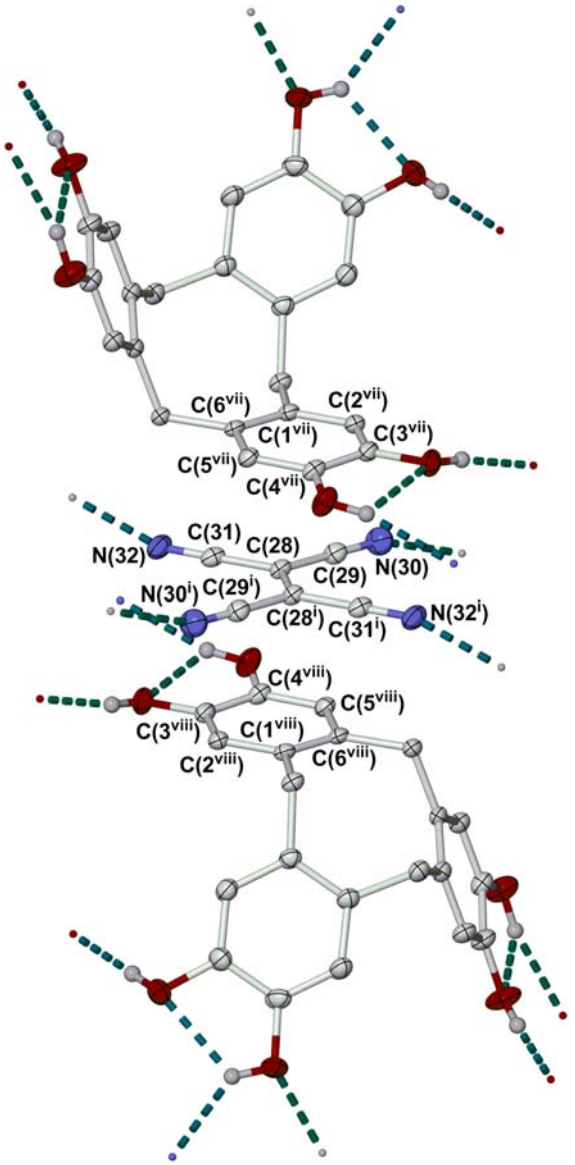

Figure 3. View of one of the two unique charge-transfer interactions between CTC and TCNE in **1**. For clarity the C-bound H atoms have been omitted, and only the atoms involved in the $\pi\cdots\pi$ interactions have been labelled. Displacement ellipsoids are at the 50% probability level. See Table 2 for the definitions of the symmetry codes.

(110) plane, with the CTC molecules being three-connected and the TCNE molecules four-connected (Figure 2). The resultant hydrogen bond topology is equivalent to McMahon's net (*24*), containing five-membered rings with $(5^3)^2 5^4 5^3 5^4$ connectivity in the short Schläfli notation (*25*). Two of the six THF molecules occupy the cavities of the CTC hosts, oriented so that the plane of their five-membered rings lies roughly co-parallel with one of the CTC phenylene groups (Figure 3). There are no C—H···O or C—H···π contacts between the included THF and CTC significantly shorter than the sum of the van der Waals radii of those groups, however.

In addition to hydrogen bonding, there are strong $\pi{\cdot}\pi$ interactions between the CTC and different TCNE molecules, related by translation along the unit cell *x*-axis (Figure 3). The TCNE forms an exclusion complex with the CTC and lies between phenylene groups from two different CTC molecules. This donor–acceptor–donor sandwich motif is common in crystalline TCNE…arene complexes (*26*). The two unique $\pi\cdots\pi$ interactions in the crystal have near-identical geometries (Table 3), the interacting groups being almost coplanar and separated by 3.099(5)–3.109(5) Å. These $\pi\cdots\pi$ interactions link the hydrogen-bonded sheets in (Figure 2) into a 3D lattice. The C═C bond lengths in the two TCNE molecules in the lattice [1.380(4) and 1.382(4) Å] are at the high end of the range usually observed for donor–acceptor complexes of this alkene, being close to the values expected for the monoanion $[TCNE]^{\cdot-}$ (*13*). The dimensions of the catechyl groups complexed to the TCNE are consistent with the catechol oxidation level, however, indicating that formal CTC → TCNE electron transfer has not taken place (*27*). Although there may be a 0.01–0.02 Å shortening of the C—O bonds in **1** compared to **3**–**6**, which would be consistent with partial catechylene oxidation, this is of borderline statistical significance. Nonetheless, the dimensions of the TCNE molecules, and the short distance between the $\pi\cdots\pi$ stacked TCNE and phenylene residues (Table 3), are both consistent with a particularly strong donor–acceptor interaction between TCNE and CTC.

Discussion of the hydrogen bonding in **2** is complicated by disorder in at least four, and probably five, of the six hydroxyl proton positions in the CTC molecule. Each disordered hydroxyl group donates hydrogen bonds

Table 3. Metric parameters for the CTC…cyanoalkene π–π interactions in **1** and **2** (Å, °).

	Dihedral angle	Interplanar spacing	Horizontal offset
$[CTC]_2{\cdot}TCNE{\cdot}6THF$ (**1**)			
$[C(1^{vii})\text{-}C(6^{vii})]\cdots[C(28)—N(32), C(28^{i})—N(32^{i})]$	2.21(6)	3.109(5)	0.21
$[C(33^{vii})—C(38^{vii})]\cdots[C(60)—N(64), C(60^{ii})—N(64^{ii})]$	1.85(6)	3.099(5)	0.16
$[CTC]_2{\cdot}TCNQ{\cdot}4THF$ (**2**)			
$[C(1^{xv})—C(6^{xv})]\cdots[C(28)—N(35), C(28^{ix})—N(35^{ix})]$	4.30(11)	3.238(14)	0.79[a]

Note: See Table 2 for the definitions of the symmetry codes, and Figures 3 and 5 for the atom numbering schemes employed in these structures.
[a] Offset from the centre of the TCNQ quinoidal C═C double bond, C(29)—C(31) (Figure 5).

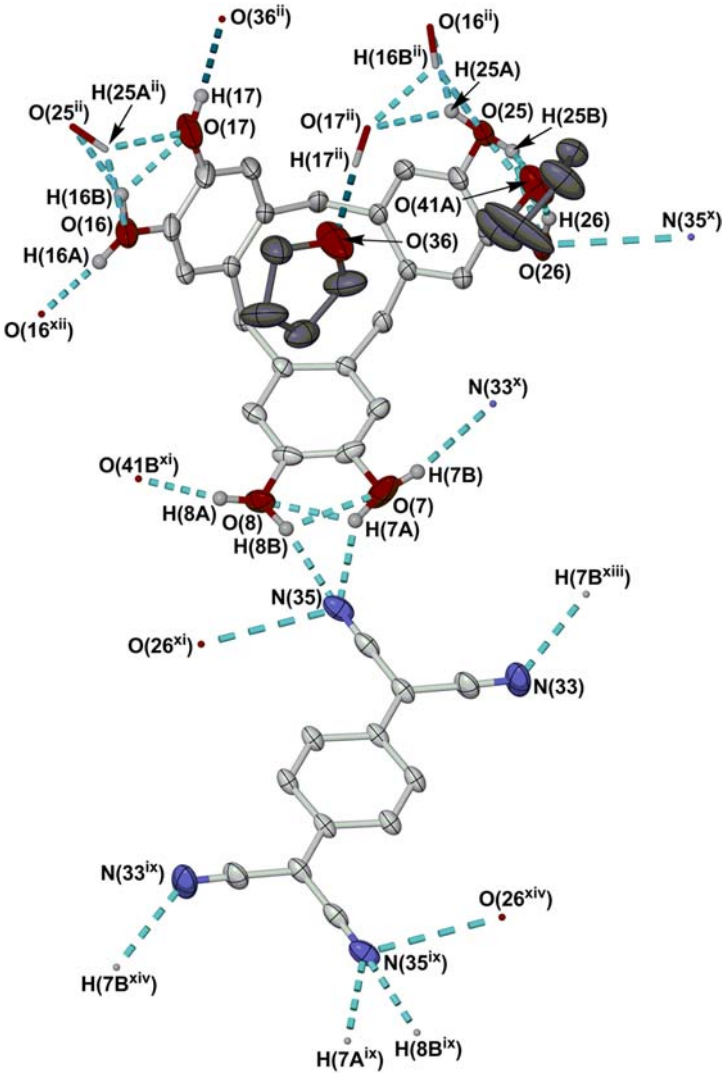

Figure 4. View of the asymmetric unit of **2**, showing the hydrogen bonding interactions in the crystal. Only the major orientation of the disordered THF molecule is shown, but both disorder sites for the hydroxyl protons are given and the disordered hydrogen bonds are shown with a paler colouration. See Table 2 for the definitions of the symmetry codes. Other details are as for Figure 1.

to two different acceptors in the lattice (Figure 4). This disorder is a consequence of the hydrogen bond O(16)—H(16)···O(16^{xii}), which requires that hydroxyl group to be disordered about the crystallographic twofold axis (Figure 4). The TCNQ molecule again has crystallographic inversion symmetry. Two of its four cyano groups [N(35) and its symmetry equivalent] accept one full hydrogen bond, which is however disordered between the two O—H donors of one catechyl ring (Figure 4). The four N atoms also accept one longer, partially occupied hydrogen bond each from other neighbouring CTC molecules. These partial hydrogen bonds link the CTC and TCNQ molecules into a 3D network, although the disorder precludes a detailed discussion of its topology. The solvent molecules occupy rectangular channels in this network, running parallel to c with dimensions 5.4 × 3.2 Å.

The TCNQ acceptor is sandwiched between two CTC catechyl rings in a staggered arrangement, with each CTC overlying one of the two C═C double bonds in the molecule (Figure 5). The $\pi\cdots\pi$ interaction between CTC and TCNQ is weaker than in **1**, according to their interplanar distance which is 0.13–0.14 Å longer in **2** than in **1** (Table 3). The internal dimensions of the TCNQ molecule, as characterised by the difference between the benzo C—C [av. 1.452(4) Å] and quinoidal C═C [1.387(2) Å] bond lengths, are consistent with a neutral TCNQ molecule (*28*), while the geometry of the complexed catechyl group is identical to those in **1** within experimental error, and is again consistent with an unoxidised catechol derivative (*27*). Therefore, as in **1**, formal CTC → TCNQ electron transfer has not taken place in **2**.

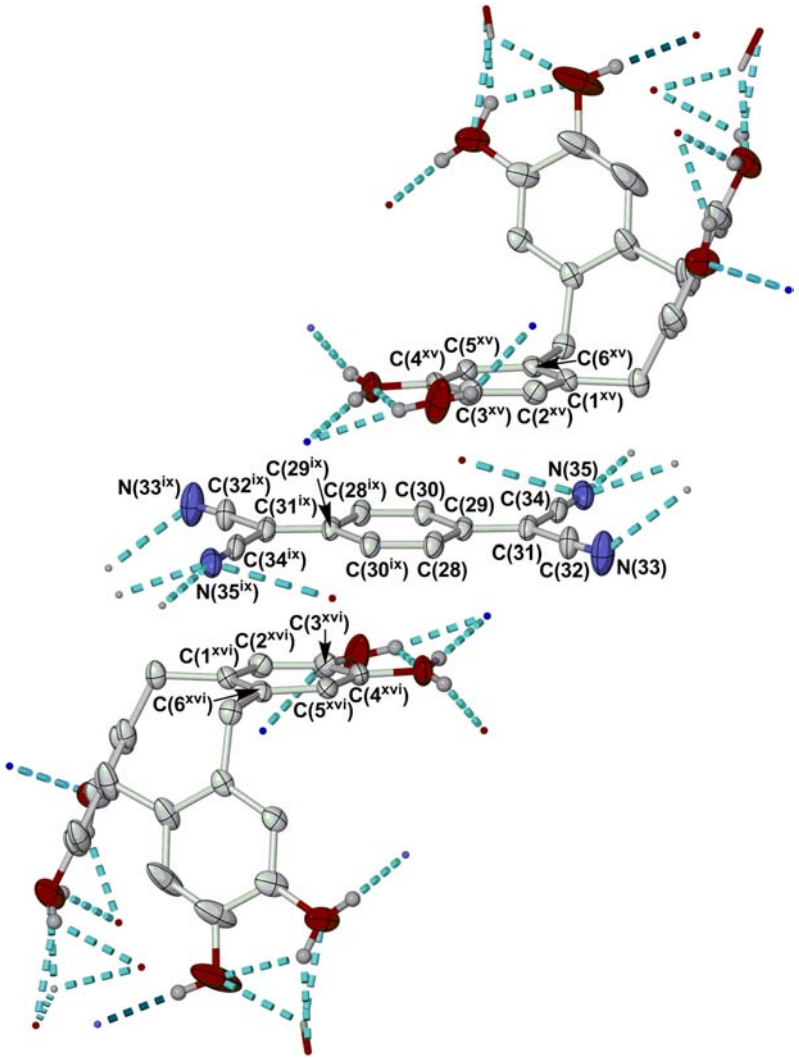

Figure 5. View of the charge-transfer interaction between CTC and TCNQ in **2**. Details are as for Figures 3 and 4.

Elemental microanalyses of **1** and **2** imply that both compounds retain most of their solvent on drying, although partial replacement of the THF solvent by atmospheric moisture appears to take place. Their IR spectra show $\nu_{C\equiv N}$ vibrations typical of donor–acceptor complexes of TCNE and TCNQ at 2249 and 2220 cm^{-1}(**1**) and 2219 cm^{-1} (**2**) (*13*, *14*). An additional weaker peak at 2238 cm^{-1} is also observed for **1**, which is not usually resolved in TCNE adducts and may be a consequence of the strong hydrogen bonding to the TCNE residue. The positive ion ES mass spectra of **1** and **2** from THF solution are essentially identical and contain peaks arising from CTC (as its sodium complexes) only. The negative ion ES mass spectra of **1** under the same conditions does provide some evidence for the association between CTC and TCNE under these conditions, via a moderate intensity mass peak assignable to $[(CTC)(TCNE) + H]^-$ (*m/z* 495.1). The negative ion ES mass spectra of **2** is dominated by peaks from $[TCNQ]^-$ and its hydrolysis product. The visible charge-transfer maximum for **1** in THF (λ_{max} 655 nm) is close to the wavelength expected for a complex between TCNE and a 4,5-dialkylcatechol residue (*29*).

Compound **3** is unique in CTC clathrate chemistry, in not forming a lattice comprised of essentially planar hydrogen-bonded networks (*4–7*). Rather, the CTC molecules associate with hydrogen bonding into an S-shaped sheet network undulating along the unit cell *b*-direction. The hydrogen bond topology within the sheets is $3^3 4^2$, with each CTC node being five-connected. Only two of the four THF sites take part in this hydrogen bonding, with one of these molecules also being included into the CTC cavities in a similar manner to that in **1** and **2**. The two other solvent sites are disordered, one of them apparently containing a mixture of water (which hydrogen bonds to CTC)" and THF (which does not). This partial water occupancy has no effect on the topology of the hydrogen bond network, however. Neighbouring CTC sheets related by translation along *a* combine to form

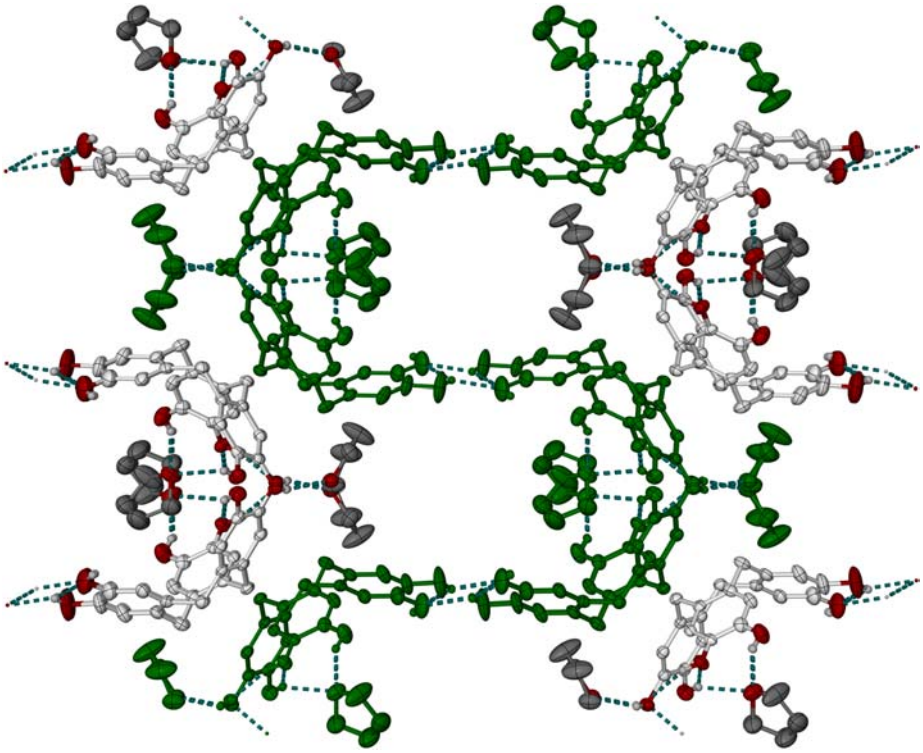

Figure 6. Partial packing diagram of **3**, showing the pores in the lattice. Only the crystallographically ordered THF molecules are shown. The view is perpendicular to the (001) crystal plane. Displacement ellipsoids are at the 50% probability level, and all C-bound H atoms have been omitted for clarity.

rectangular pores running parallel to (001), of approximate dimensions 15.0 × 7.5 Å (Figure 5). The walls of the pores also contain additional voids, of around 7.5 × 6.0 Å. Opposite sides of the pores are lined by ordered THF molecules, hydrogen bonded to the walls of the channels (Figure 6), while the disordered solvent environments lie at the centre of the channels and in the voids.

Three other solvates of CTC were also isolated during the course of this work, from attempts to co-crystallise CTC with cyanoalkene acceptors where the solution bleached during the crystallisation process. Crystalline CTC·2EtOH (**4**) is isomorphous with previously reported CTC·2^{i}PrOH (*5*), and adopts the same hydrogen bonding connectivity. This leads to the bilayered packing motif adopted by most previously reported CTC clathrate crystals (Figure 7) (*4–6*) with one of the two unique ethanol molecules lying sideways in the CTC cavity. There is no direct hydrogen bond between a CTC molecule and its included ethanol guest, but the two are linked by two hydrogen bond pathways involving bridging hydroxyl groups from neighbouring CTC molecules. Each CTC molecule is six-connected in its hydrogen bond topology if connections through bridging ethanol molecules are included, forming a $3^3 4^4$ network within the bilayer structure. The same overall network connectivity is also exhibited by CTC·2^{i}PrOH (*5*) and CTC·DMSO (*4*), although the pattern of hydrogen bonding in the latter structure is different from **4**.

Although they are not isomorphous, the clathrate CTC·3DMA (DMA, dimethylacetamide; **5**) adopts the alternative hydrogen-bonded *bis*-monolayer structure type found in CTC·2DMF·2H_2O (*7*). Molecules in the CTC monolayers in **5** are related by translational symmetry, giving rise to a simple 4^4 hydrogen bonding connectivity if pathways through bridging DMA molecules are included. Adjacent monolayers are related by crystallographic C_2 axes, leading to bilayers of CTC molecules encapsulating sheets of DMA solvent (Figure 7). The solvent molecules within these sheets are crystallographically ordered, being held in place by hydrogen bonds to the CTC walls. One of the two unique DMA environments in the solvent sheets protrudes into the CTC cavity (related by $-1/2 + x$, $1/2 - y$, $-1/2 + z$). One *N*-methyl group of the included DMA molecule is directed towards the centre of the base of the CTC host, and is in van der Waals contact with the bases of two of its phenylene groups. There are again no short C—H···O or C—H···π contacts between the guest molecule and the CTC, however.

Finally, CTC·5DMSO (DMSO, dimethylsulphoxide; **6**) is a pseudopolymorph of the previously published 1:1 CTC·DMSO solvate (*4*). Its CTC molecules associate with chains parallel to the unit cell *a*-axis, through a pattern of

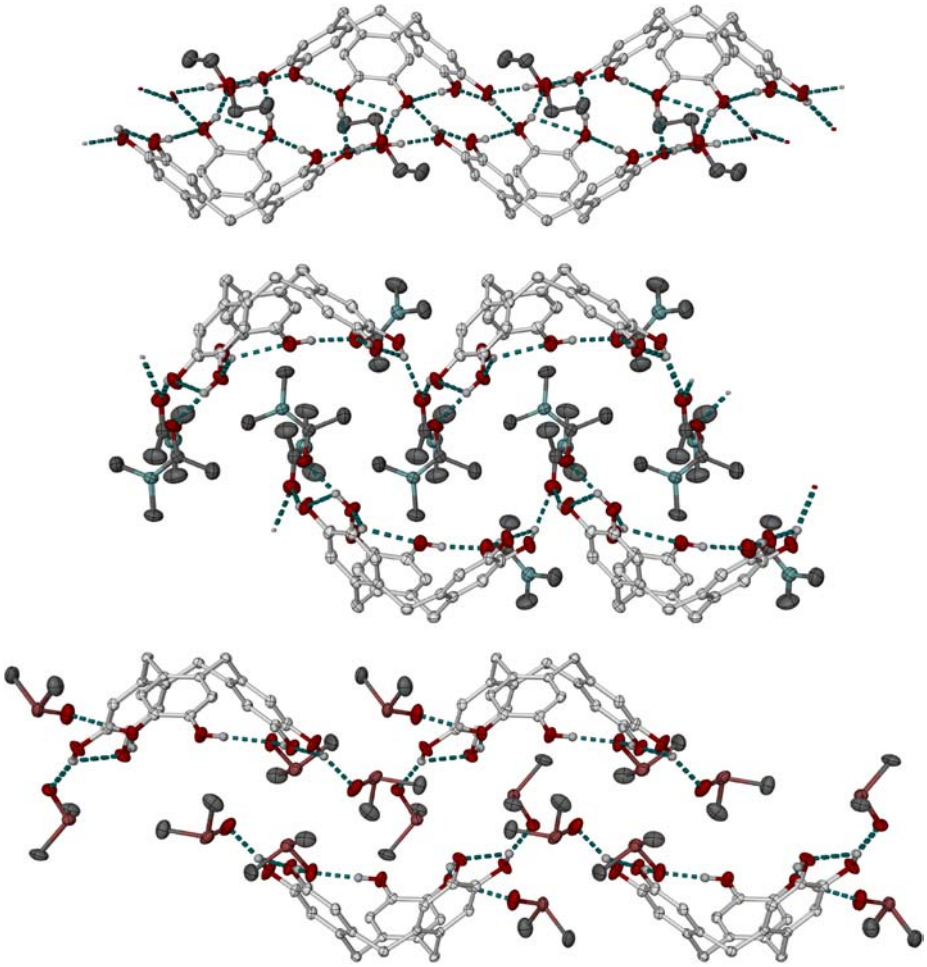

Figure 7. Partial packing diagrams of the clathrates **4**–**6**. Top: the hydrogen-bonded bilayer network in **4**. Centre: the *bis*-monolayer motif in **5**. Bottom: the chains of CTC molecules in **6**, looking down the direction of the chains. Displacement ellipsoids are at the 50% probability level, and all C-bound H atoms have been omitted for clarity.

hydrogen bonds that is also present in the monolayers in **5**. However, rather than associating further into two dimensions, the chains in **6** are well separated from each other by additional hydrogen-bonded DMSO molecules. The lattice in **6** contains sheets of DMSO molecules that are encapsulated by layers of CTC, formed by translation of the CTC chains along *c* (Figure 7). One of the DMSO molecules is included into the CTC cavities, as before. This arrangement again has clear similarities to that found in **5** (Figure 7).

Conclusion

Compounds **1** and **2** are noteworthy for several reasons. They are the first crystallographically characterised complexes of an organic cavitand host with a cyanoalkene electron acceptor (*16*–*19*). Notably the solid state structures of **1** and **2** are consistent with a previous study of a resorcinarene:TCNE adduct, which was proposed to be an exclusion complex on the basis of a semi-empirical calculation (*17*). In addition, **1** and **2** represent the first structure determinations of TCNE or TCNQ complexes of a catechol, and of TCNE with any phenol derivative (*29*–*31*); a small number of TCNQ/phenol co-crystals are known (*32*). Finally, they are rare examples of the neutral TCNE (*33*) and TCNQ (*34*) molecules (as opposed to their radical anions) acting as classical hydrogen bond acceptors; **1** is the first such material where TCNE accepts more than two hydrogen bonds. The IR and UV–vis spectra of **1** and **2** resemble those of TCNE and TCNQ complexes with catechol itself (*29*, *30*) and other polyhydroxybenzenes (*31*). These imply a significant degree of charge transfer between the arene donor and TCNE acceptor, although not to the extent of formal ionisation of these groups.

The formula of **5** is consistent with a previous spectroscopic determination of CTC clathrates, which predicted a 1:3 stoichiometry for the CTC:DMA adduct as observed in this work (*5*). The literature structures of CTC·2^{i}PrOH (*5*) and CTC·2acetone (*6*) also agree with

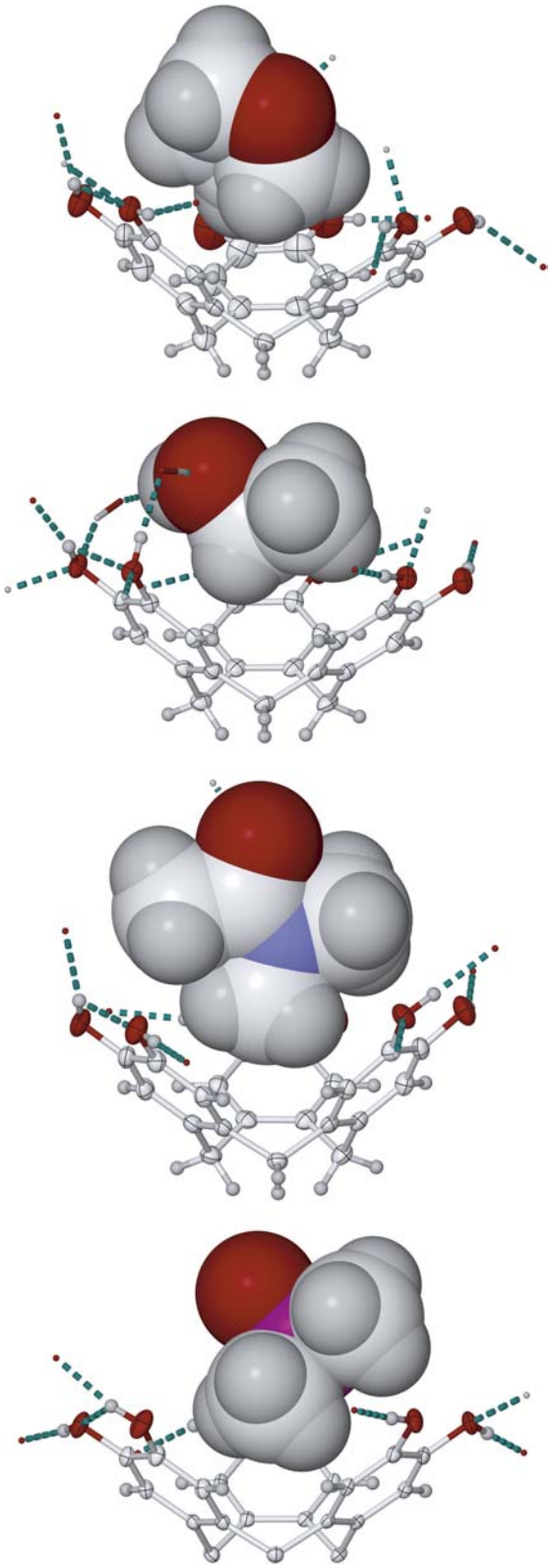

Figure 8. Views of the included solvent molecules in the CTC clathrates in this work, from top to bottom: THF in **3**; EtOH in **4**; DMA in **5**; and, DMSO in **6**. Displacement ellipsoids for the CTC moieties are at the 50% probability level.

their stoichiometries from the same study, while it may also be relevant that the stoichiometry predicted for the CTC:DMSO complex (1:3) is the average of the stoichiometry of **6** (1:5) and the previously published 1:1 CTC·DMSO solvate (*4*). Our isolation of **4** contrasts with the results in Ref. (*5*), however, which reported no association between ethanol and CTC in the crystal, while Ref. (*5*) did not analyse the CTC/THF solvate.

Finally, it is striking that every compound in this work and nearly all the CTC-containing structures in the literature (*4*–*8*) contain solvent molecules included in the host cavity (Figure 8). That contrasts with CTV derivatives, which tend to self-associate in the crystal through a 'handshake' motif, involving in-cavity $\pi\cdots\pi$ interactions between neighbouring CTV molecules that preclude the inclusion of exogenous guests (*2*, *7*, *35*, *36*). Of the solvents known to be bound by CTC, only DMF appears to include within the cavities of CTV derivatives with any regularity (*36*, *37*). In contrast, while there are more than 150 organic or metal-organic CTV derivatives on the Cambridge Crystallographic Database (*38*), only one of these (a cryptophane cage) has included THF (*39*), two (also cage structures) included DMSO (*10*), and one (a metallated derivative) included acetone (*40*). Notably, there are no direct hydrogen bonds between a CTC molecule and its included solvent in any of its clathrate structures, and the guest molecule is only bound inside the cavity by weak C—H$\cdots\pi$, van der Waals and/or hydrophobic interactions. Therefore, the increased affinity for guest inclusion by CTC is probably a function of its preferred modes of self-association in the solid state with hydrogen bonding, which leave the cavity unobstructed for guest binding.

Supplementary material available

Crystallographic data for the structures reported in this paper have been deposited with the Cambridge Crystallographic Data Centre, as supplementary publications Nos. CCDC 830757 (**1**), 830761 (**2**), 830762 (**3**), 830758 (**4**), 830759 (**5**) and 830760 (**6**).

Acknowledgement

This work was funded by the EPSRC.

References

(1) (a) Collet, A. *Tetrahdron* **1987**, *43*, 5725–5759; (b) Hardie, M.J.; Nichols, P.J.; Raston, C.L. *Adv. Supramol. Chem.* **2002**, *8*, 1–41.
(2) Hardie, M.J. *Chem. Soc. Rev.* **2010**, *39*, 516–527.
(3) Brotin, T.; Dutasta, J.-P. *Chem. Rev.* **2009**, *109*, 88–130.
(4) Chakrabarti, A.; Chawla, H.M.; Hundal, G.; Pant, N. *Tetrahedron* **2005**, *61*, 12323–12329.

(5) Hyatt, J.A.; Duesler, E.N.; Curtin, D.Y.; Paul, I.C. *J. Org. Chem.* **1980**, *45*, 5074–5079.
(6) Sumby, C.J.; Hardie, M.J. *Acta Cryst. Sect. E* **2007**, *63*, o1537–o1539.
(7) Steed, J.W.; Zhang, H.; Atwood, J.L. *Supramol. Chem.* **1996**, *7*, 37–45.
(8) Bohle, D.S.; Stasko, D. *Chem. Commun.* **1998**, 567–568.
(9) (a) Abrahams, B.F.; FitzGerald, N.J.; Hudson, T.A.; Robson, R.; Waters, T. *Angew. Chem. Int. Ed.* **2009**, *48*, 3129–3132; (b) Abrahams, B.F.; FitzGerald, N.J.; Robson, R. *Angew. Chem. Int. Ed.* **2010**, *49*, 2896–2899; (c) Abrahams, B.F.; Boughton, B.A.; FitzGerald, N.J.; Holmes, J.L.; Robson, R. *Chem. Commun.* **2011**, *47*, 7404–7406.
(10) (a) Ronson, T.K.; Fisher, J.; Harding, L.P.; Rizkallah, P.J.; Warren, J.E.; Hardie, M.J. *Nat. Chem.* **2009**, *1*, 212–216; (b) Ronson, T.K.; Carruthers, C.; Fisher, J.; Brotin, T.; Harding, L.P.; Rizkallah, P.J.; Hardie, M.J. *Inorg. Chem.* **2010**, *49*, 675–685.
(11) For other recent references see: (a) Carruthers, C.; Fisher, J.; Harding, L.P.; Hardie, M.J. *Dalton Trans.* **2010**, *39*, 355–357; (b) Little, M.A.; Halcrow, M.A.; Harding, L.P.; Hardie, M.J. *Inorg. Chem.* **2010**, *49*, 9486–9496; (c) Ronson, T.K.; Nowell, H.; Westcott, A.; Hardie, M.J. *Chem. Commun.* **2011**, *47*, 176–178; (d) Henkelis, J.J.; Ronson, T.K.; Harding, L.P.; Hardie, M.J. *Chem. Commun.* **2011**, *47*, 6560–6562.
(12) Pierpont, C.G.; Lange, C.W. *Prog. Inorg. Chem.* **1994**, *41*, 331–442.
(13) Miller, J.S. *Angew. Chem. Int. Ed.* **2006**, *45*, 2508–2525.
(14) Kaim, W.; Moscherosch, M. *Coord. Chem. Rev.* **1994**, *129*, 157–193.
(15) (a) Fatiadi, A.J. *Synthesis* **1987**, 959–978; (c) Ballester, L.; Gutiérrez, A.; Perpiñán, M.F.; Azcondo, M.T. *Coord. Chem. Rev.* **1999**, *190–192*, 447–470; (d) Hünig, S.; Herberth, E. *Chem. Rev.* **2004**, *104*, 5535–5563.
(16) Ikeda, A.; Nagasaki, T.; Araki, K.; Shinkai, S. *Tetrahedron* **1992**, *48*, 1059–1070.
(17) Urbaniak, M.; lwanek, W. *Tetrahedron* **1999**, *55*, 14459–14466.
(18) Pietraszkiewicz, O.; Koźbiał, M.; Pietraszkiewicz, M. *Adv. Mater. Opt. Electron.* **1998**, *8*, 277–284.
(19) Ogoshi, T.; Kitajima, K.; Umeda, K.; Hiramitsu, S.; Kanai, S.; Fujinami, S.; Yamagishi, T.; Nakamoto, Y. *Tetrahedron* **2009**, *65*, 10644–10649.
(20) Sheldrick, G.M. *Acta Cryst. Sect. A* **2008**, *64*, 112–122.
(21) Barbour, L.J. *J. Supramol. Chem.* **2001**, *1*, 189–191.
(22) Spek, A.L. *J. Appl. Cryst.* **2003**, *36*, 7–13.
(23) Cehak, A.; Chyla, A.; Radomska, M.; Radomski, R. *Mol. Cryst. Liq. Cryst.* **1985**, *120*, 327–331.
(24) O'Keefe, M.; Hyde, B.G. *Philos. Trans. R. Soc. Lond. A* **1980**, *295*, 553–618.
(25) Carlucci, L.; Ciani, G.; Proserpio, D.M. *Coord. Chem. Rev.* **2003**, *246*, 247–289.
(26) See e.g. (a) Larsen, F.K.; Little, R.G.; Coppens, P. *Acta Cryst. Sect. B* **1975**, *31*, 430–440; (b) Cohen-Addad, C.; Lebars, M.; Renault, A.; Baret, P. *Acta Cryst. Sect. C* **1984**, *40*, 1927–1931; (c) Renault, A.; Cohen-Addad, C. *Acta Cryst. Sect. C* **1986**, *42*, 1529–1533; (d) Colonna, B.; Menzer, S.; Raymo, F.M.; Stoddart, J.F.; Williams, D.J. *Tetrahedron Lett.* **1998**, *39*, 5155–5158; (e) Haderski, G.J.; Chen, Z.; Krafcik, R.B.; Masnovi, J.; Baker, R.J.; Towns, R.L.R. *J. Phys. Chem. B* **2000**, *104*, 2242–2250; (f) Le Maguères, P.; Lindeman, S.V.; Kochi, J.K. *J. Chem. Soc. Perkin Trans. 2* **2001**, 1180–1185; (g) Arrais, A.; Boccaleri, E.; Croce, G.; Milanesio, M.; Orlando, R.; Diana, E. *Cryst. Eng. Comm.* **2003**, *5*, 388–394; (h) Pawlukojć, A.; Sawka-Dobrowolsk, W.; Bator, G.; Sobczyk, L; Grech, E.; Nowicka-Scheibe, J. *Chem. Phys.* **2006**, *327*, 311–318..
(27) Carugo, O.; Castellani, C.B.; Djinović, K.; Rizzi, M. *J. Chem. Soc. Dalton Trans.* **1992**, 837–841.
(28) Moore, A.J.; Bryce, M.R.; Batsanov, A.S.; Heaton, J.N.; Lehmann, C.W.; Howard, J.A.K.; Robertson, N.; Underhill, A.E.; Perepichka, I.F. *J. Mater. Chem.* **1998**, *8*, 1541–1550.
(29) Frey, J.E.; Aiello, T.; Beaman, D.N.; Combs, S.D.; Fu, S.-L.; Puckett, J.J. *J. Org. Chem.* **1994**, *59*, 1817–1830.
(30) (a) Beukers, R.; Szent-Gyorgyi, A. *Recl. Trav. Chim. Pays-Bas* **1962**, *81*, 255–268; (b) Spange, S.; Maenz, K.; Stadermann, D. *Liebigs Annal.* **1992**, 1033–1037.
(31) Reddy, A.R.; KrishnaMurthy, N.V.; Bhudevi, B. *Spectrochim. Acta A* **2006**, *63*, 700–708.
(32) (a) Inabe, T.; Okaniwa, K.; Okamoto, H.; Mitani, T.; Maruyama, Y.; Takeda, S. *Mol. Cryst. Liq. Cryst. Sci. Tech. Sect. A* **1992**, *216*, 229–234; (b) Bentiss, F.; Lagrenee, M.; Mentre, O.; Wignacourt, J.P.; H.Vezin, H.; Holt, E.M. *J. Mol. Struct.* **2002**, *607*, 31–41..
(33) (a) Castellano, E.E.; Rivero, B.E.; Podjarny, A.D.; Roselli, M.E. *Acta Cryst. Sect. B* **1980**, *36*, 1726–1728; (b) Bocelli, G.; Cardellini, L.; de Meo, G.; Ricci, A.; Rizzoli, C.; Tosi, G. *J. Cryst. Spectrosc. Res.* **1990**, *20*, 561–569; (c) Masnovi, J.; Baker, R.J.; Towns, R.L.R.; Chen, Z. *J. Org. Chem.* **1991**, *56*, 176–179; (d) Delgado, S.; Muñoz, A.; Medina, M.E.; Pastor, C.J. *Inorg. Chim. Acta* **2006**, *359*, 109–117..
(34) (a) Yakushi, K.; Ikemoto, I.; Kuroda, H. *Acta Cryst. Sect. B* **1974**, *30*, 835–837; (b) Yakushi, K.; Ikemoto, I.; Kuroda, H. *Acta Cryst. Sect. B* **1974**, *30*, 1738–1742; (c) Inabe, T.; Okaniwa, K.; Ogata, H.; Okamoto, H.; Mitani, T.; Maruyama, Y. *Acta Chim. Hung.* **1993**, *130*, 537–534; (d) Alibadi, M.A.M.; Batsanov, A.S.; Bramham, G.; Charmant, J.P.H.; Haddow, M.F.; MacKay, L.; Mansell, S.M.; McGrady, J.E.; Norman, N.C.; Roffey, A.; Russell, C.A. *Dalton Trans.* **2009**, 5348–5354.
(35) Caira, M.R.; Jacobs, A.; Nassimbeni, L.R. *Supramol. Chem.* **2004**, *16*, 337–342.
(36) Carruthers, C.; Ronson, T.K.; Sumby, C.J.; Westcott, A.; Harding, L.P.; Prior, T.J.; Rizkallah, P.; Hardie, M.J. *Chem. Eur. J.* **2008**, *14*, 10286–10296.
(37) See e.g. (a) Hardie, M.J.; Raston, C.L. *Cryst. Growth Des.* **2001**, *1*, 53–58; (b) Mough, S.T.; Holman, K.T. *Chem. Commun.* **2008**, 1407–1409; (c) Sumby, C.J.; Gordon, K.C.; Walsh, T.J.; Hardie, M.J. *Chem. Eur. J.* **2008**, *14*, 4415–4425.
(38) Allen, F.H. *Acta Cryst. Sect. B* **2002**, *58*, 380–388.
(39) Mough, S.T.; Goeltz, J.C.; Holman, K.T. *Angew. Chem. Int. Ed.* **2004**, *43*, 5631–5635.
(40) Hancock, K.S.B.; Steed, J.W. *Chem. Commun.* **1998**, 1409–1410.